

Vacuolar H⁺-ATPase c Protects Glial Cell Death Induced by Sodium Nitroprusside Under Glutathione-Depleted Condition

Yu Jeong Byun,¹ Seong-Beom Lee,² Hwa Ok Lee,¹ Min Jeong Son,¹ Ho-Shik Kim,¹ Oh-Joo Kwon,¹ and Seong-Whan Jeong^{1*}

¹Department of Biochemistry, College of Medicine, The Catholic University of Korea, 505 Banpo-dong, Seocho-gu, Seoul 137-701, Korea

²Department of Pathology, College of Medicine, The Catholic University of Korea, 505 Banpo-dong, Seocho-gu, Seoul 137-701, Korea

ABSTRACT

We examined the role of the c subunit (ATP6L) of vacuolar H⁺-ATPase and its molecular mechanisms in glial cell death induced by sodium nitroprusside (SNP). ATP6L siRNA-transfected cells treated with SNP showed a significant increase in cytotoxicity under glutathione (GSH)-depleted conditions after pretreatment with buthionine sulfoximine, but reduction of ATP6L did not affect the regulation of lysosomal pH in analyses with lysosomal pH-dependent fluorescence probes. Photodegraded SNP and ferrous sulfate induced cytotoxicity with the same pattern as that of SNP, but SNAP and potassium cyanide did not show activity. Pretreatment of the transfected cells with deferoxamine (DFO) reduced ROS production and significantly inhibited the cytotoxicity, which indicates that primarily iron rather than nitric oxide or cyanide from SNP contributes to cell death. Involvement of apoptotic processes in the cells was not shown. Pretreatment with JNK or p38 chemical inhibitor significantly inhibited the cytotoxicity, and we also confirmed that the MAPKs were activated in the cells by immunoblot analysis. Significant increase of LC3-II conversion was observed in the cells, and the conversions were inhibited by cotransfection of the MAPK siRNAs and pretreatment with DFO. Introduction of Atg5 siRNA inhibited the cytotoxicity and inhibited the activation of MAPKs and the conversion of LC3. We finally confirmed autophagic cell death and involvement of MAPKs by observation of autophagic vacuoles via electron microscopy. These data suggest that ATP6L has a protective role against SNP-induced autophagic cell death via inhibition of JNK and p38 in GSH-depleted glial cells. *J. Cell. Biochem.* 112: 1985–1996, 2011. © 2011 Wiley-Liss, Inc.

KEY WORDS: ATP6L; SODIUM NITROPRUSSIDE; GLUTATHIONE; AUTOPHAGY; MAPK; GLIA

Nitric oxide (NO) is a free radical with an unpaired electron, and it reacts with superoxide anion to generate peroxynitrite, a highly reactive molecule that is potentially damaging to proteins and DNA [Mancardi et al., 2004]. Reactive nitrogen species (RNS) are directly linked to reactive oxygen species (ROS), and mammalian cells maintain ROS/RNS at low levels through antioxidant systems, such as superoxide dismutase (SOD), vitamins E and C, and glutathione (GSH) [Reiter, 1995; Son et al., 2010]. Sodium nitroprusside (SNP) is a water-soluble complex consisting of a ferrous ion surrounded by five cyanide (CN) moieties and one NO. SNP has been used clinically as a powerful vasodilator for treatment of cardiac failure and all forms of hypertensive emergencies, and in basic research it has been used to investigate the cell death

mechanisms triggered under conditions of NO-induced stress [Friederich and Butterworth, 1995; Kawasaki et al., 2007].

Although NO is a well-known molecule responsible for many toxicological effects elicited by SNP, several studies showed that many biological properties of SNP are independent of the NO moiety and are due to the release of iron and CN during its decomposition. For example, studies demonstrated that induction of heme oxygenase-1 expression and iron regulatory protein 2 degradation by SNP is tightly dependent on the iron moiety not NO from the SNP [Kim et al., 2006; Wang et al., 2006]. Furthermore, it was reported that ROS generation by the iron moiety rather than NO from SNP is implicated in the mechanism of cardiomyocyte and neural cell death [Rauhala et al., 1998; Rabkin and Kong, 2000; Cardaci et al., 2008]. It

Grant sponsor: Korea Science and Engineering Foundation (KOSEF) through the MRC for Cell Death Disease Research Center (CDDRC); Grant number: R13-2002-005-03002-0.

*Correspondence to: Seong-Whan Jeong, MD, PhD, Department of Biochemistry, College of Medicine, The Catholic University of Korea, 505 Banpo-dong, Seocho-gu, Seoul 137-701, Korea. E-mail: swjeong@catholic.ac.kr

Received 29 December 2010; Accepted 9 March 2011 • DOI 10.1002/jcb.23105 • © 2011 Wiley-Liss, Inc.

Published online 23 March 2011 in Wiley Online Library (wileyonlinelibrary.com).

was demonstrated that SNP is a redox-active iron moiety containing a free iron coordination site for H₂O₂ that can lead to the generation of ROS via the Fenton reaction [Ramakrishna Rao and Cederbaum, 1996].

GSH is the most abundant and important antioxidant for protecting cells from damage induced by ROS. Depletion of cellular GSH with buthionine sulfoximine (BSO), an inhibitor of γ -glutamylcysteine synthetase, enhances the cytotoxic effects that are associated with elevated production of ROS [Zeevalk et al., 1998; Dringen, 2000]. Glial cells seem to play a role in protecting neurons from oxidative stress by establishing an anti-oxidative defense system [Makar et al., 1994] because GSH is more abundant within astrocytes [Halliwell, 1992]. Recent report, however, showed that astrocytes are more sensitive to hydrogen peroxide than neurons in dissociated cell cultures of hippocampal slices and the cytotoxicity was inhibited by pretreatment with antioxidants [Feeney et al., 2008]. In our previous study, depletion of GSH with BSO significantly enhanced cytotoxicity by treatment of osteoblasts and glial cells with oxidative stresses [Byun et al., 2007; Son et al., 2010].

We have confirmed a gene, the c subunit (ATP6L) of vacuolar H⁺-ATPase, that exhibits changes in gene expression under oxidative stress [Byun et al., 2007]. The vacuolar H⁺-ATPase (V-ATPase) is a widely distributed ATP-dependent proton pump that acidifies intracellular compartments (lysosomes, trans-Golgi cisternae, endosomes, secretory vesicles, etc.), and it is a large multisubunit complex composed of 14 polypeptides and organized into cytoplasmic (V₁) and transmembrane (V₀) domains. ATP6L is a component of six different subunits in the V₀ domain. It was reported that overexpression of ATP6L in fibroblasts enhances the invasion activity of the cells [Kubota and Seyama, 2000]. Furthermore, ATP6L has been found to be associated with E5 oncoprotein and β 1 integrin, which indicates a role of ATP6L in cell growth and differentiation [Andresson et al., 1995; Skinner and Wildeman, 1999]. We demonstrated that ATP6L has a protective role against H₂O₂-induced cell death via an inhibition of the Erk1/2 signaling pathway in C6 glial cells under GSH-depleted conditions [Byun et al., 2007]. These data suggest that ATP6L has functions independent of its role as part of the V-ATPase complex. In this study, we examined the role of ATP6L and its molecular mechanisms in glial cell death induced by SNP.

MATERIALS AND METHODS

MATERIALS

Dulbecco's modified Eagle's medium (DMEM) and fetal bovine serum (FBS) were purchased from Thermo Scientific (Waltham, MA). LysoTracker Red DND-99, LysoSensor Green DND-153, and 2',7'-dichlorodihydrofluorescein diacetate (H₂DCF-DA) were from Invitrogen (Carlsbad, CA). SNP (Na₂[Fe(CN)₅NO]), ferrous sulfate (FeSO₄), potassium hexacyanoferrate (III) (K₃[Fe(CN)₆]), potassium cyanide (KCN), S-nitro-N-acetylpenicillamine (SNAP, C₇H₁₂N₂O₄S), deferoxamine mesylate (DFO), 2-phenyl-4,4,5,5-tetramethylimidazole-1-oxyl-3-oxide (PTIO), bafilomycin A1, 3-methyladenine (3-MA), and BSO were from Sigma-Aldrich (St. Louis, MO). Wortmannin, SB202190, SP600125, and tempol were from Calbiochem (San

Diego, CA), and zVAD-fmk was from Tocris Bioscience (Ellisville, MO). 3-(4,5-Dimethylthiazol-2-yl)-2, 5-diphenyltetrazolium bromide (MTT) was from Duchefa (Haarlem, Netherlands). RNAzol was from Tel-Test (Friendswood, TX). AccuPowerTM CycleScript and 2 \times SYBR[®] Premix Ex TaqTM were from TaKaRa Bio, Inc. (Shiga, Japan). The ApoScan Annexin V-FITC apoptosis detection kit was from BioBud (Seoul, Korea). Antibodies against LC3B, p-JNK, p-cJun, p-p38, p38, beclin-1, caspase-3, and PARP were from Cell Signaling Technology (Beverly, MA). The GAPDH antibody was from Santa Cruz Biotechnology (Santa Cruz, CA). The Atg5 antibody was from MBL (Nagoya, Japan), and the JNK antibody was from Upstate (Billerica, MA). The β -actin antibody and secondary mouse and rabbit antibodies were from Sigma. The PVDF membrane and ECLTM Western Blotting Detection Reagents were from GE Healthcare (Buckinghamshire, England); ImmobilonTM Western was from Millipore (Billerica, MA).

CELL CULTURE, siRNA TRANSFECTION, AND CELL VIABILITY ASSAY

C6 glioma cells (ATCC, Rockville, MD) were cultured in DMEM supplemented with 10% FBS at 37°C in 5% CO₂/95% air. An SNP solution was prepared by dissolving the powder in water. Photodegraded SNP (SNP_{ex}) was obtained by exposing the SNP solution to light for two days at room temperature. Cells were transfected with small interfering RNAs (siRNAs) targeted for each gene using a microporator (Invitrogen) at 1,700 V and 20 ms according to the manufacturer's instruction [Byun et al., 2007]. After 24 h, the cells were seeded into 96-well plates at 0.7 \times 10⁴ cells per well in medium containing 100 μ M BSO, the concentration used in our previous work [Byun et al., 2007]. After culture for an additional 24 h, the cells were treated with various concentrations of SNP with 100 μ M BSO for 6 h. Cell viability was analyzed by MTT reduction assay. The cell viability assay also was performed following pretreatment with MAPK inhibitors or chemicals 1 h before addition of SNP. The inhibitors or chemicals used were SB202190 (p38 inhibitor), SP600125 (JNK/SAPK inhibitor), Wortmannin (PI3K inhibitor), zVAD-fmk (pan-specific caspase inhibitor), PTIO (NO scavenger), DFO (iron chelator), and tempol (ROS scavenger). The duplex siRNA ATP6L-1: 5'-GAACAACCCCGAAUAUUCU-3', ATP6L-2: 5'-CCAUCAUCCAGUGGUUAU-3', and Atg5: 5'-ACCGGAAACUCAUGGAAUA-3' were synthesized by Ambion (Austin, TX). JNK-1, JNK-2, p38, and negative control siRNA were purchased from Ambion. Beclin-1 siRNA was from Dharmacon (Lafayette, CO). Efficiency in silencing gene expression was determined 2 days after transfection by immunoblot or real-time reverse transcription PCR (RT-PCR). Cell viabilities were expressed as a percentage of that observed in untreated cells. Effect on cell viability by the silencing siRNAs was compared with that in cells transfected with a non-silencing siRNA control.

REVERSE TRANSCRIPTION AND QUANTITATIVE REAL-TIME RT-PCR

To validate the expression level of ATP6L, a quantitative real-time RT-PCR was performed using the cDNA as a template and the specific primer sets. Total RNA was isolated from cells at the indicated conditions using RNAzol according to the manufacturer's instructions. Two micrograms of total RNA from each sample were reverse transcribed to cDNA using an AccuPowerTM CycleScript. The

primer pairs used were ATP6L forward: 5'-GGCCAGAGCTGATCAT-GAAG-3' and ATP6L reverse: 5'-CACCAGCATCTCCGACAATG-3'. The amplification was performed using an Mx3000P system (Stratagene, La Jolla, CA) in a 25 μ l reaction mixture containing 2 μ l of diluted cDNA templates, 5 pmol of each primer, and 12.5 μ l of 2 \times SYBR[®] Premix Ex Taq[™] including ROX dye. GAPDH was used to normalize the expression levels of each sample. The relative mRNA level of ATP6L was calculated using the $2^{-\Delta\Delta C_t}$ method [Livak and Schmittgen, 2001].

MEASUREMENT OF LYSOSOMAL ACIDITY

LysoTracker Red DND-99 is a fluorescent acidotropic probe and accumulates in lysosomes and acidic organelles [Santic et al., 2008]. LysoSensor Green DND-153 exhibits a pH-dependent increase in fluorescence intensity upon neutralization [Lin et al., 2001]. Cells were collected 2 days after transfection with siRNA. The cells were washed twice in PBS and incubated for 5 min at 37°C with PBS containing 50 nM LysoTracker Red DND-99 or 1 μ M LysoSensor Green DND-153 according to the manufacturer's instructions. Fluorescence was immediately determined by flow cytometry using 590-nm emission in the cells stained with LysoTracker Red DND-99 or 505-nm emission filter in the cells stained with LysoSensor Green DND-153 (FACSCalibur, Becton Dickinson, San Jose, CA) and analyzed using CellQuest software (Becton Dickinson). As a control experiment of pH changes in lysosomes, lysosomal pH also was measured in non-transfected cells pretreated with 100 nM bafilomycin A1 1 h before addition of the fluorescence probes. The fluorescent intensity in the ATP6L siRNA-transfected cells was compared with that in the control siRNA-transfected cells and non-transfected cells pretreated with bafilomycin A1.

DETECTION OF INTRACELLULAR ROS

Detection of intracellular ROS including RNS was performed as described previously [Son et al., 2010]. To visualize intracellular ROS generation at the end of treatment, cells were incubated for 10 min with 5 μ M H₂DCF-DA, which primarily reacts with hydroxyl radical and peroxynitrite [Keller et al., 2004]. The cells were washed with PBS, and DCF fluorescence intensity was monitored using a fluorescence microscope (IX71, Olympus, Tokyo, Japan). To determine the intracellular ROS levels, the fluorescence intensities emitted at 504–525 nm from the suspended cells incubated with 5 μ M H₂DCF-DA were measured using a flow cytometer (FACSCalibur) and analyzed using CellQuest software (Becton Dickinson). The fluorescent intensity in the cells transfected with ATP6L siRNA was compared to that in the cells transfected with control siRNA.

FLOW CYTOMETRIC ANALYSIS OF APOPTOSIS

Determination of apoptosis was performed using an ApoScan Annexin V-FITC apoptosis detection kit according to the manufacturer's protocol, as described previously [Jang et al., 2009]. The siRNA-transfected cells were treated with SNP for 2 h, and the cells were collected and washed twice in PBS. The cells were incubated for 15 min at room temperature with annexin V-FITC, and propidium iodide (PI) was added. The cells were immediately acquired using flow cytometry at a wavelength of 518 and 620 nm, and analyzed using CellQuest software.

IMMUNOBLOT ANALYSIS

On the second day of transfection, cells were treated with 5 μ M SNP. After incubation of indicated times, cells were harvested and lysed with 1 \times SDS-PAGE loading buffer. Equal amounts of cell lysates were loaded and separated by SDS-PAGE, and proteins were transferred to PVDF membranes. The membranes were incubated with primary antibodies; next, they were incubated with secondary antibodies conjugated to horseradish peroxidase. Immunoreactive protein signals were visualized using ECL[™] Western Blotting Detection Reagents or Immobilon[™] Western. β -actin or GAPDH were used as internal controls in the immunoblot analysis. The levels of proteins loaded were quantified by densitometry using an LAS-3000 (Fuji Film, Tokyo, Japan), and equal amounts of protein were determined. The conversion of LC3 was expressed in the ratio of LC3-II to LC3-I determined by densitometry of the immunoblots. Immunoblots also were performed following pretreatment with DFO 1 h before the addition of SNP.

TRANSMISSION ELECTRON MICROSCOPY

On the second day of transfection, cells were treated with 5 μ M SNP. After 2 h incubation, the cells were fixed with 2.5% glutaraldehyde for 2 h, postfixed in 1% osmium tetroxide, dehydrated in ethanol, and embedded in Epon 812. Ultrathin sections were contrasted with uranyl acetate and lead citrate. Sections were examined using a JEM 1010 CX transmission electron microscope (JEOL, Arishima, Japan).

STATISTICAL ANALYSIS

Analysis and graphing of data were done with Prism 4.0 (GraphPad Software, San Diego, CA). Data are expressed as means \pm SEM of at least three independent experiments. Statistical analysis was performed by two-way ANOVA for multiple group comparisons followed by Bonferroni posttests. A value of $P < 0.05$ was considered statistically significant.

RESULTS

ATP6L ON SNP-INDUCED GLIAL CYTOTOXICITY IN GSH-DEPLETED CONDITION

Our previous report suggests that change of ATP6L expression may be important in the response to various oxidative stresses. In this study, we examined the role of ATP6L and its molecular mechanisms in C6 glial cell death induced by SNP. To examine the molecular mechanisms in cell death, we introduced ATP6L siRNA into the cells by microporation to silence gene expression. Two types of ATP6L siRNAs tested were efficient in silencing gene expression to approximately 20–30% that of control siRNA 2 days after transfection, as determined via real-time RT-PCR (Fig. 1A). The ATP6L protein could not be clearly identified with immunoblot analysis using commercial ATP6L antibodies in the rat C6 glial cells. We, therefore, evaluated the effects of ATP6L siRNAs through real-time RT-PCR. ATP6L siRNA-1 was used in all the following experiments. Without pretreatment with BSO, the change of cytotoxicity in the ATP6L siRNA-transfected cells treated with SNP was not shown in the cell viability assay (Fig. 1B). After overnight pretreatment with BSO, ATP6L siRNA-transfected cells treated with SNP showed a significant, dose-dependent increase in

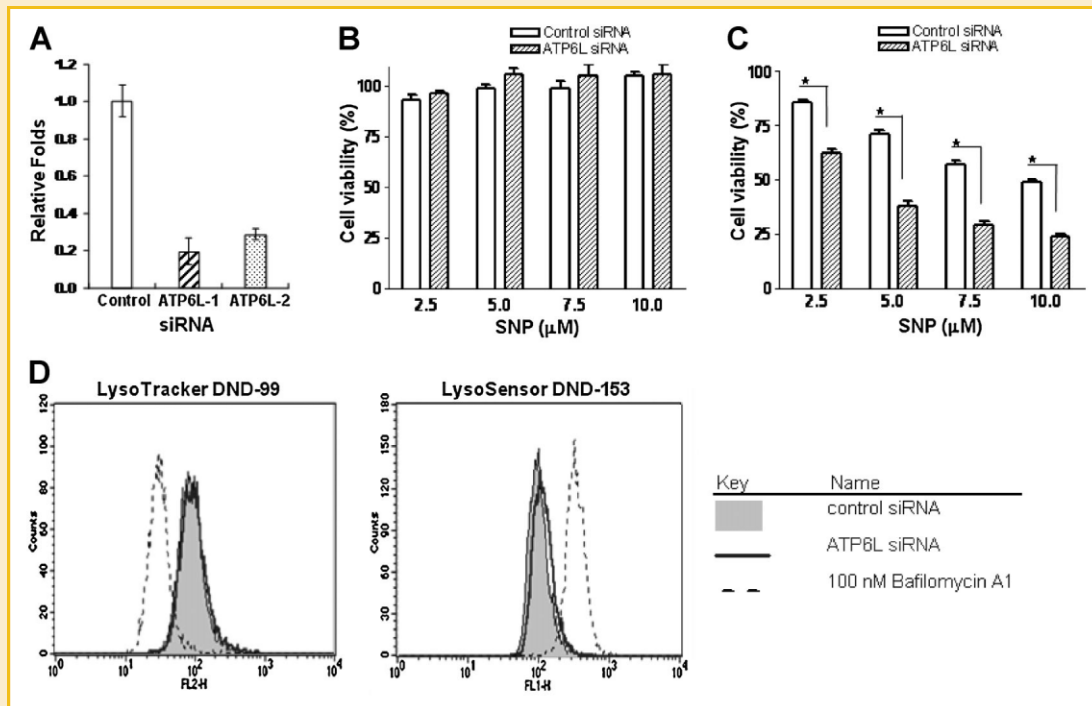


Fig. 1. Increase of sodium nitroprusside (SNP)-induced cytotoxicity by silencing gene expression of the vacuolar H^+ -ATPase c subunit (ATP6L) in glutathione (GSH)-depleted C6 glial cells. A: siRNAs were transfected into C6 glial cells by microporation, and efficiency of silencing ATP6L expression was examined with real-time RT-PCR 48 h after transfection. The transfected cells were treated with various concentrations of SNP for 6 h in the absence (B) or presence (C) of buthionine sulfoximine (BSO). Cell viability was determined by an MTT reduction assay. The data represent the mean \pm SEM of 26 independent experiments. * $P < 0.05$ versus the values in control siRNA-transfected cells (two-way ANOVA, Bonferroni posttests). D: The changes of pH in lysosomes were monitored with two fluorescence probes. The cells were collected 2 days after transfection with siRNAs and incubated with LysoTracker Red DND-99 or LysoSensor Green DND-153. Fluorescence in the cells was immediately determined by flow cytometry. As a control experiment, non-transfected cells were pretreated with bafilomycin A1 1 h before addition of the fluorescence probes.

cytotoxicity compared to that of cells transfected with a control non-silencing siRNA (Fig. 1C). The following experiments were performed under GSH-depleted conditions with BSO pretreatment. In the assay, SNP was applied to cells at concentrations ranging from 0 to 10 μ M. In a previous study, we showed that the intracellular level of GSH was dose-dependently reduced after treatment with BSO [Byun et al., 2009]. The GSH level in cells treated with 100 μ M BSO was negligible compared with that of non-treated cells.

V-ATPase is a large multi-subunit complex protein, and it is important in pH regulation of intracellular organelles. LysoTracker Red DND-99 probe exhibits a pH-dependent decrease in fluorescence intensity upon lysosomal acidification [Santic et al., 2008], and LysoSensor Green DND-153 probe exhibits a pH-dependent increase in fluorescence intensity upon lysosomal neutralization [Lin et al., 2001]. The two fluorescence probes have been used to monitor changes in the pH of lysosomal vesicles (Fig. 1D). Bafilomycin A1 is a specific inhibitor of the ability of V-ATPase to inhibit acidification of organelles [Crider et al., 1994]. Cells treated with bafilomycin A1 showed a decrease of LysoTracker Red DND-99 probe fluorescence intensity and an increase of the LysoSensor Red DND-153 intensity, which indicates normal function of proton pump V-ATPase in regulation of the lysosomal pH. ATP6L siRNA-transfected cells incubated with the fluorescence probes showed no change in fluorescence intensity compared to that of

control siRNA-transfected cells. The data imply that reduction of cellular ATP6L by the transfection of ATP6L siRNA did not affect regulation of lysosomal pH via the proton pump V-ATPase. These data suggest that ATP6L plays roles independent of the V-ATPase protein complex in SNP-induced cytotoxicity under GSH-depleted conditions.

CONTRIBUTIONS OF IRON MOIETY OF SNP TO CYTOTOXICITY RATHER THAN NO OR CN

Decomposition of SNP in culture media generates NO, iron, and CN. However, it is unclear which molecule is responsible for the SNP-induced cytotoxicity in ATP6L siRNA-transfected cells. Although NO is considered the active component of SNP, an increasing number of reports indicate that several SNP-elicited cellular effects are NO independent [Kim et al., 2006; Wang et al., 2006]. To determine the actual mediator of SNP-induced cell death, we used photodegraded SNP (SNP_{ex}) that has exhausted its capacity for NO release and retains redox-active iron [Rauhala et al., 1998]. Unexpectedly, SNP_{ex} and ferrous sulfate induced cytotoxicity with the same patterns as that of SNP (Fig. 2A-C). To further evaluate NO or CN effects of SNP on cytotoxicity, cells were treated with CN (potassium hexacyanoferrate and potassium cyanide) or an NO (SNAP) donor. Cell viabilities were not affected by the compounds in ATP6L siRNA-transfected cells compared to those of control siRNA-

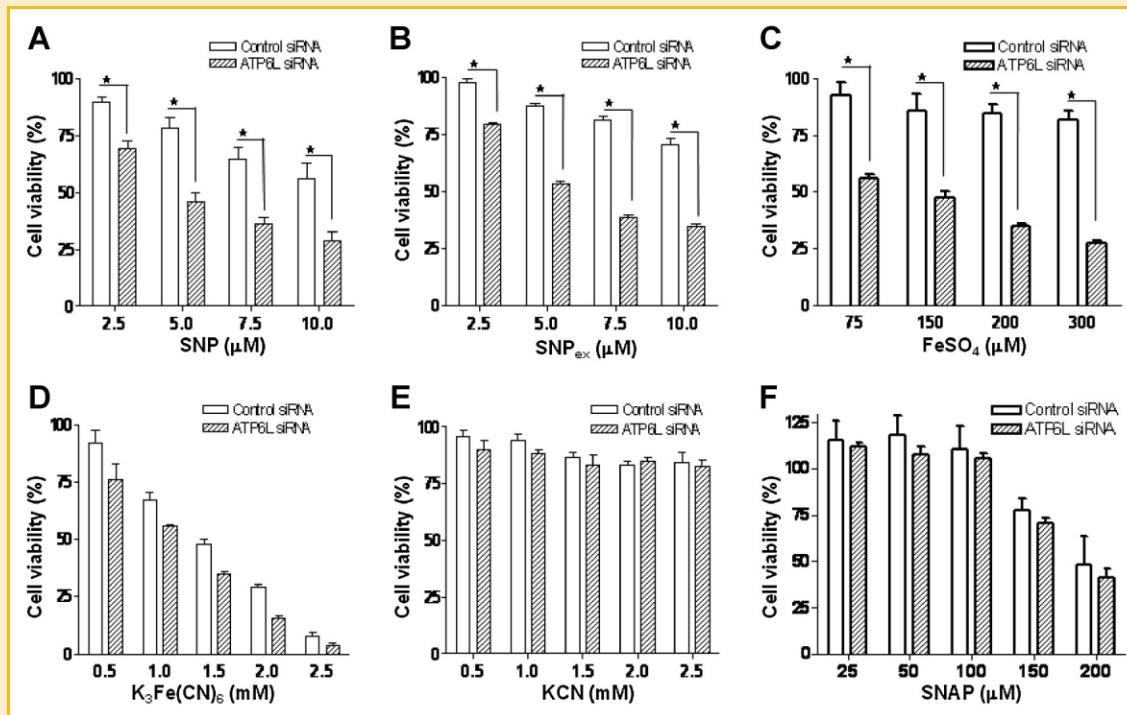


Fig. 2. Contribution of the iron moiety—rather than nitric oxide (NO) or cyanide (CN) derived from SNP—to cytotoxicity in ATP6L siRNA-transfected cells. The cells transfected with control or ATP6L siRNA were treated with various concentrations of SNP (A), SNP_{ex} (B), FeSO₄ (C), K₃Fe(CN)₆ (D), KCN (E), or SNAP (F) in the presence of BSO. Cell viability was determined via an MTT reduction assay. The data represent the mean ± SEM of four independent experiments. **P* < 0.05 versus the values in control siRNA-transfected cells.

transfected cells (Fig. 2D–F). However, pretreatment of the transfected cells with DFO, an iron chelator, completely inhibited the cytotoxicity (Fig. 3B). Pretreatment with PTIO, a NO scavenger, inhibited the cytotoxicity with less degree compared to that with DFO. These data demonstrate that iron rather than NO or CN from SNP dominantly contributes to cytotoxicity in ATP6L siRNA-transfected cells under GSH-depleted conditions.

SNP-INDUCED ROS RESPONSIBLE FOR CYTOTOXICITY

Indeed, it was demonstrated that during its redox cycling, SNP is able to trigger the generation of ROS, mainly hydroxyl radicals, via the Fenton reaction [Ramakrishna Rao and Cederbaum, 1996]. Since iron released from SNP was responsible for cytotoxicity in the ATP6L siRNA-transfected cells, we examined whether or not SNP addition correlates with the generation of ROS, including RNS. We measured the intracellular ROS accumulation by staining cells with H₂DCF-DA. Significant increase of DCF fluorescence was shown in ATP6L siRNA-transfected cells after SNP treatment for 2 h via flow cytometry analysis (Fig. 3A). The increase of fluorescence in the cells was inhibited by pretreatment with DFO. Direct observation of the cells with fluorescence microscope showed the corresponding results to that with flow cytometer (data not shown). And pretreatment of the cells with tempol, a ROS scavenger, inhibited the cytotoxicity (Fig. 3B). These data suggest that ROS generated by the iron component of SNP are responsible for the cytotoxicity in

ATP6L siRNA-transfected cells, and ATP6L is involved in regulation of intracellular ROS levels.

NON-APOPTOTIC CELL DEATH BY SNP VIA JNK AND P38 MAPK ACTIVATION

With confirmation of its protective role, we examined the effects of ATP6L on signaling pathways involved in SNP-induced cytotoxicity. It is widely recognized that MAPK pathways are important in the regulation of cell survival and death in response to intracellular ROS levels. First of all, cell viability was examined in ATP6L siRNA-transfected cells by pretreatment with MAPK inhibitors (Fig. 4A). Pretreatment of the cells with a PI3K inhibitor (Wortmannin) had no effect on the cytotoxicity, but pretreatment with a p38 (SB202190) or JNK (SP600125) inhibitor significantly inhibited the cytotoxicity. As shown in Figure 5, we also confirmed via immunoblot analysis that JNK and p38 MAPKs were activated in ATP6L siRNA-transfected cells treated with SNP for 2 h. These data suggest that ATP6L has a protective role against SNP-induced cell death through inhibition of JNK and p38 MAPKs.

To examine whether or not the SNP-induced cytotoxicity was attributed to apoptosis, ATP6L siRNA-transfected cells treated with SNP were analyzed by staining with annexin V and propidium iodide in flow cytometry. Apoptotic rates were quite low in both control and ATP6L siRNA-transfected cells (Fig. 4B). We further examined the cytotoxicity with molecular apoptotic markers. We could not detect the cleavage fragments of procaspase-3 and PARP

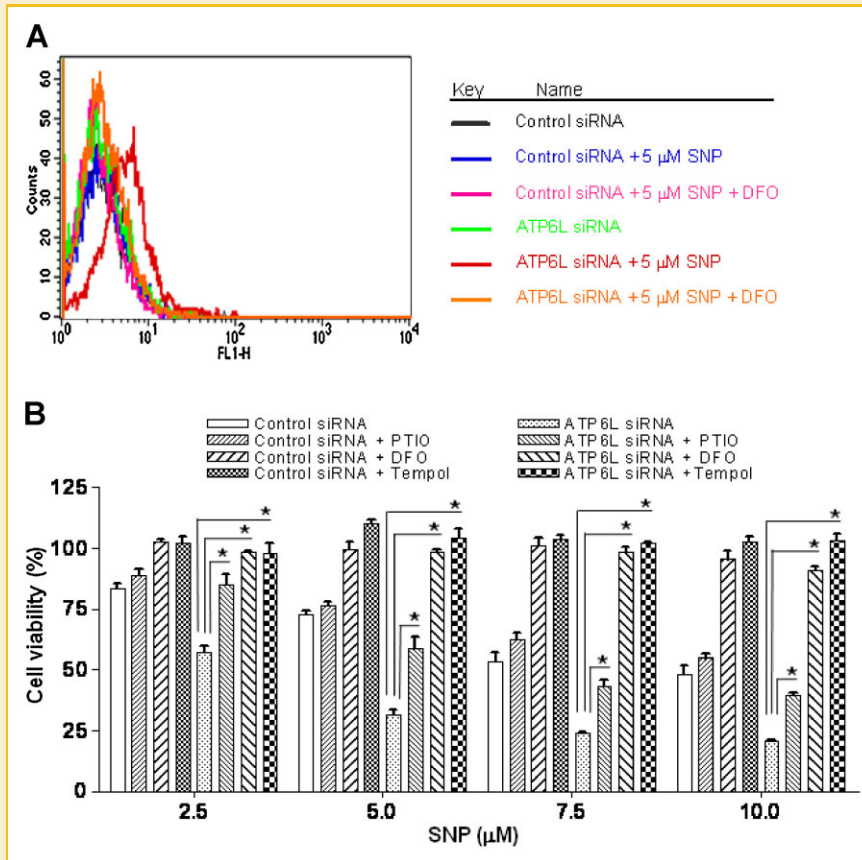


Fig. 3. Contribution of iron-induced reactive oxygen species (ROS) derived from SNP to cytotoxicity in ATP6L siRNA-transfected cells. A: Iron-induced ROS generation in ATP6L siRNA-transfected cells treated with SNP was determined. siRNA-transfected cells were treated with 5 μ M SNP for 2 h in the presence of BSO without or with pretreatment with 20 μ M deferoxamine (DFO). The cells were incubated with 5 μ M H₂DCF-DA, and fluorescence intensities were measured in flow cytometry, as described in the Materials and Methods Section. B: siRNA-transfected cells were treated with SNP in the presence of BSO without or with pretreatment with 20 μ M PTIO, 20 μ M deferoxamine (DFO), and 5 μ M tempol. Cell viability was determined by an MTT reduction assay. The data represent the mean \pm SEM of four independent experiments. * P < 0.05 versus the values in ATP6L siRNA-transfected cells without pretreatment.

in immunoblot analyses (Fig. 4C), and pretreatment with zVAD-fmk, a pan-specific caspase inhibitor, had no effect on SNP-induced cytotoxicity in the cells (Fig. 4A). The data suggest that SNP-induced cytotoxicity in the ATP6L siRNA-transfected cells is shown primarily in non-apoptotic.

INVOLVEMENT OF ROS, JNK, AND P38 IN SNP-INDUCED AUTOPHAGIC CELL DEATH

We were unable to observe any involvement of apoptotic processes in ATP6L siRNA-transfected cells treated with SNP. We, therefore, examined the autophagic process in cells treated with SNP. To identify whether or not SNP induced autophagy, we observed the conversion of LC3-I into LC3-II, a marker of autophagy, by immunoblot. Increase of LC3-II conversion was observed in the ATP6L siRNA-transfected cells treated with SNP (Fig. 5A), and pretreatment of the cells with DFO inhibited the conversion (Fig. 5B). We have shown that pretreatment of the cells with DFO inhibited SNP-induced cytotoxicity (Fig. 3B). Significant activation of JNK and p38 MAPKs was shown in the ATP6L siRNA-transfected cells treated with SNP (Fig. 5A), and pretreatment of the cells with DFO

inhibited activation of MAPKs and conversion of LC3 (Fig. 5B). Involvement of the MAPKs in the cells corresponded to the results of the cell viability assay, as described above. Collectively these data suggest that iron-induced ROS from SNP are involved in autophagic cell death via activation of p38 and JNK MAPKs in ATP6L siRNA-transfected cells under GSH-depleted conditions.

SNP-INDUCED NON-CANONICAL AUTOPHAGIC CELL DEATH DEPENDENT UPON ATG5

We observed the activation of autophagic marker LC3 in ATP6L siRNA-transfected cells treated with SNP. Although the autophagic process was stimulated, the level of beclin-1 protein was unchanged by SNP treatment of the cells (Fig. 6A). To further confirm autophagic cell death by SNP, we introduced beclin-1 or Atg5 siRNAs into cells to silence gene expression. The siRNAs were efficient in silencing the expression of beclin-1 and Atg5 proteins (Fig. 6B). Atg5 siRNA was able to significantly inhibit cytotoxicity in ATP6L siRNA-transfected cells treated with SNP, but beclin-1 siRNA had no effect on the cytotoxicity (Fig. 6C). Pretreatment of the cells with 3-MA, a PI3K inhibitor, did not affect cytotoxicity either. These

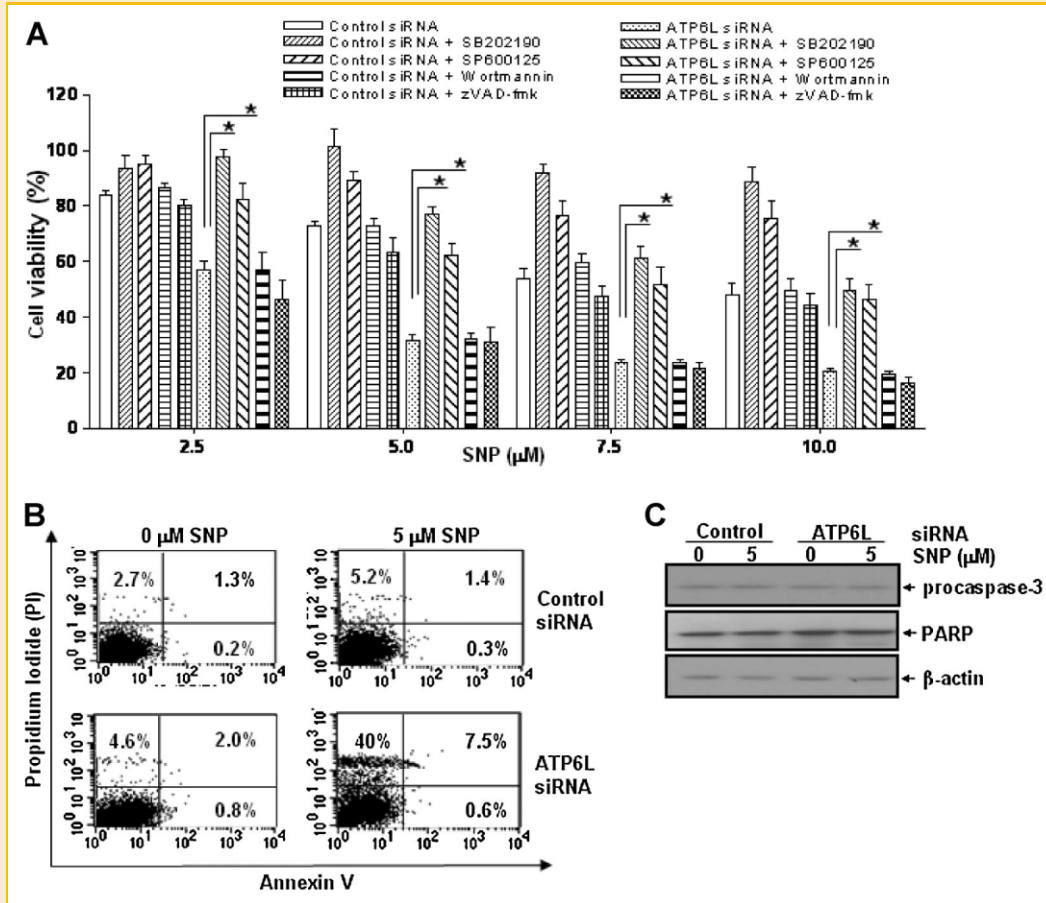


Fig. 4. SNP-induced non-apoptotic cell death via JNK and p38 MAPKs in ATP6L siRNA-transfected cells. A: siRNA-transfected cells were treated with SNP in the presence of BSO without or with pretreatment with chemical inhibitors. The inhibitors are 20 μ M SB202190 (p38), 20 μ M SP600125 (JNK), 200 nM Wortmannin (PI3K), and 20 μ M zVAD-fmk (pan-specific caspase). Cell viability was determined by an MTT reduction assay. The data represent the mean \pm SEM of four independent experiments. * P < 0.05 versus the values in ATP6L siRNA-transfected cells without pretreatment. B: siRNA-transfected cells were treated with SNP for 2 h in the presence of BSO. The cells were stained with annexin V and propidium iodide (PI) and analyzed by flow cytometry, as described in the Materials and Methods Section. C: The siRNA-transfected cells treated with 5 μ M SNP for 2 h were lysed, and caspase-3 and PARP proteins were examined by immunoblot analysis of the lysates. β -actin was used as a loading control.

data suggest that SNP triggers non-canonical autophagic cell death in ATP6L siRNA-transfected cells under GSH-depleted conditions.

INVOLVEMENT OF P38 AND JNK IN PROCESSES OF AUTOPHAGIC CELL DEATH

In ATP6L siRNA-transfected cells treated with SNP, we have shown the activation of p38 and JNK and the inhibition of cytotoxicity with pretreatment of the cells with a p38 or JNK chemical inhibitor. The activation patterns of MAPKs were coincident with LC3 conversion. To further examine the molecular mechanisms, we introduced the p38 and JNK siRNAs into cells to silence gene expression. p38 and JNK siRNAs were efficient in silencing gene expression (Fig. 7A). p38 and JNK1 siRNAs were able to significantly inhibit cytotoxicity (Fig. 7B) and LC3 conversion (Fig. 8A,B) in the ATP6L siRNA-transfected cells treated with SNP. Conversely, JNK2 siRNA had no effect on cell viability (Fig. 7B). Interestingly, we observed that cointroduction of Atg5 and ATP6L siRNAs into cells inhibited the activation of p38 and JNK, and it inhibited the conversion of LC3 in immunoblot analyses (Fig. 8B). These results suggest that activation

of p38 or JNK in ATP6L siRNA-transfected cells treated with SNP occurred after initiation of the autophagic process. But we could not observe any evidence of interactions between p38 and JNK activation in the immunoblot analyses. The ultrastructural morphology of the ATP6L siRNA-transfected cells was examined using transmission electron microscopy to confirm autophagic cell death and the role of MAPKs (Fig. 8C). Numerous cytoplasmic autophagic vacuoles with double membranes were observed in the ATP6L siRNA-transfected cells treated with SNP, which were inhibited by cotransfection of Atg5, p38, or JNK1 siRNA. These data suggest that ATP6L has a protective role in autophagic cell death induced by SNP via inhibition of p38 and JNK MAPKs in GSH-depleted glial cells.

DISCUSSION

Evidence for crucial roles of glial cells in mechanical and metabolic support for neuronal functions has been described. Glial cells are much more than support neurons in the central nervous system

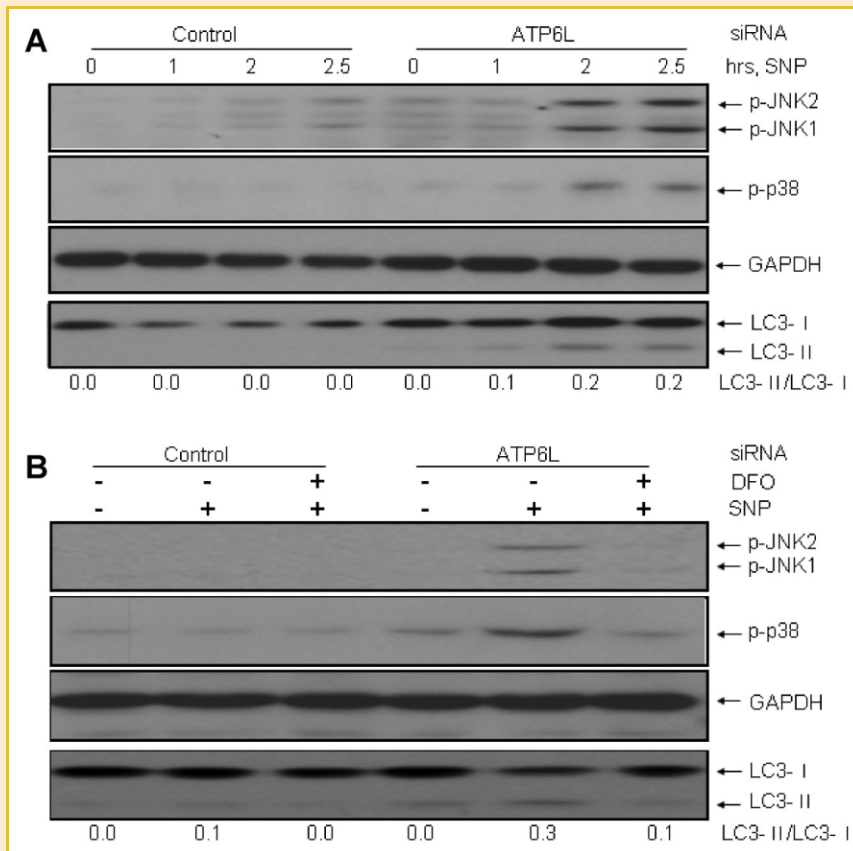


Fig. 5. Activation of JNK and p38 MAPKs in ATP6L siRNA-transfected cells treated with SNP. siRNA-transfected cells were treated with 5 μ M SNP for indicated times (A) and the cells were treated with 5 μ M SNP for 2 h without or with pretreatment with 20 μ M deferoxamine (DFO) (B) in the presence of BSO. Phosphorylation of p38 and JNK, and conversion of LC3 were examined by immunoblot analysis. Conversion was expressed in a ratio of LC3-II to LC3-I as determined by densitometry of the immunoblots. GAPDH was used as a loading control.

[Takuma et al., 2004]. Glial cells receive inputs, assimilate information, and send instructive signals to neurons as well as to neighboring glial cells. Glial cells are also involved in the defense system of the brain against elevated ROS levels that result in oxidative damage. Recent studies, however, demonstrated that astrocytes are more vulnerable to oxidative stress than neurons in dissociated rat hippocampal cultures and intracellular GSH level decreases in the penumbral astrocytes of ischemic rat brain [Feeney et al., 2008; Bragin et al., 2010]. GSH is essential for maintaining intracellular redox homeostasis and also plays an important role in eliminating ROS. GSH depletion would contribute to the increase in production of ROS and would increase oxidative damage [Coyle and Puttfarcken, 1993; Simonian and Coyle, 1996].

In a previous study, we found that mRNA expression of ATP6L decreases in a renal ischemia/reperfusion model and increased in H₂O₂-treated C6 glioma cells [Byun et al., 2007]. We demonstrated that ATP6L siRNA-transfected cells treated with H₂O₂ show a significant increase in cytotoxicity under GSH-depleted conditions [Byun et al., 2007]. It was demonstrated that SNP can induce cytotoxicity in human glioma cells [Blackburn et al., 1998]. In this study, ATP6L siRNA-transfected cells are more vulnerable to SNP-

induced cytotoxicity than control siRNA-transfected cells under GSH-depleted conditions. This finding indicates that decrease of intracellular GSH is involved in SNP-induced cytotoxicity and that ATP6L has a protective role in cell death. It is well known that gliomas are highly resistant to radiation therapy and chemotherapeutic drugs. Therefore, it may be considered that inhibition of GSH synthesis is effective for patients undergoing radiation or chemotherapy.

ATP6L is a component of V-ATPase complex composed of 14 polypeptides. It was reported that ATP6L plays distinct roles from proton pumping. ATP6L expression is elevated in invasive breast cancer tissues, and overexpression of ATP6L in fibroblasts enhances the invasion activity of the cells [Kubota and Seyama, 2000]. ATP6L is able to bind to papillomavirus oncoprotein E5 and β 1 integrin involved in platelet derived growth factor receptor signaling, which indicates a role of ATP6L in cell growth and differentiation [Andresson et al., 1995; Skinner and Wildeman, 1999]. The binding of ATP6L to E5 protein does not affect V-ATPase activity in yeasts [Ashby et al., 2001]. But contrary results showing inhibition of organellar acidification by introduction of ATP6L siRNA and the binding of ATP6L to E5 protein were reported [Schapiro et al., 2000;

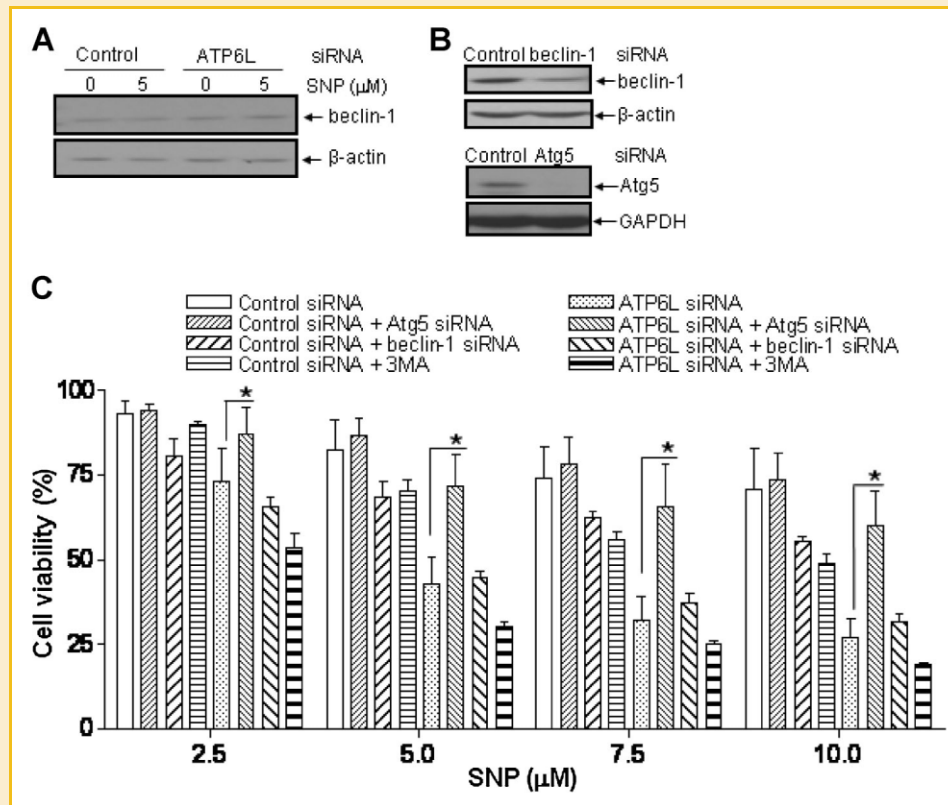


Fig. 6. SNP-induced cytotoxicity dependent on Atg5 in ATP6L siRNA-transfected cells. A: siRNA-transfected cells were treated with 5 μ M SNP for 2 h in the presence BSO. The cells were lysed, and beclin-1 was examined by immunoblot analysis of the protein lysates. β -actin was used as a loading control. B: Efficiency of silencing gene expression was examined after transfection of Atg5 or beclin-1 siRNA by immunoblot analysis of protein lysates. β -actin and GAPDH were used as loading controls. C: SNP-induced cytotoxicity was examined by coinroduction of ATP6L siRNA with Atg5 or beclin-1 siRNA into cells. The coinroduced cells were treated with SNP for 6 h in the presence of BSO. Cell viability was determined by an MTT reduction assay. Effect of pretreatment with 3MA also was examined in ATP6L-transfected cells treated with SNP. The data represent the mean \pm SEM of three independent experiments. * $P < 0.05$ versus the values in the cells transfected with ATP6L siRNA alone.

You et al., 2009]. The biological roles of ATP6L independent of V-ATPase should be studied further. In the present study, we examined whether or not contributions of ATP6L silencing to the SNP-induced cytotoxicity are proton pump-dependent functions of V-ATPase in C6 cells. With specific fluorescence probes, LysoTracker Red DND-99 and LysoSensor Green DND-153, we found no change in the lysosomal pH in ATP6L siRNA-transfected cells compared to that of control cells. We observed a 20–30% ATP6L mRNA level upon transfection of the ATP6L siRNA. The remaining ATP6L might be sufficient to maintain V-ATPase function. Taken together, our data suggest that ATP6L functions independently of its role as part of the V-ATPase protein complex in SNP-induced glial cytotoxicity under GSH-depleted conditions.

Numerous reports described the roles of each NO, iron, or CN component released from SNP, but most of them were on the main contribution of NO to cytotoxicity. In our experiment, SNP_{ex} and ferrous sulfate maintained cytotoxicity equal to that of SNP, but NO and CN donors had no activity. Furthermore, pretreatment with the iron chelator DFO completely inhibited the cytotoxicity. The data imply the contribution of iron rather than NO or CN from SNP to ROS generation in ATP6L siRNA-transfected glial cells under GSH-depleted conditions. We observed an increase in iron-induced ROS

generation with a fluorescence probe, H₂DCF-DA, and the contribution of ROS to the cytotoxicity was confirmed by pretreatment of the cells with the ROS scavenger, tempol. Evidences supporting the cytotoxicity of ROS generated by SNP have been reported. SNP_{ex} administered into the intranigral region in rats induces generation of hydroxyl radicals, leading to neurotoxicity, and exposure of the SNP_{ex} in the neuronal cell SH-SY5Y increases intracellular ROS, leading to apoptosis [Rauhala et al., 1998; Cardaci et al., 2008]. In our viability assays, pretreatment of cells with an NO scavenger (PTIO) inhibited SNP-induced cytotoxicity, but the degree of the inhibition was less than that for pretreatment with DFO. Regarding the PTIO and SNAP effects observed, it might be speculated that generation of NO-derived peroxynitrite from SNP minimally contributed to cytotoxicity. We have no data supporting any interaction between iron and NO in our experiments.

It is well known that oxidative stresses activate MAPK pathways, consequently affecting cell survival or death [Kim and Choi, 2010]. We found that p38 and JNK were activated in ATP6L siRNA-transfected cells treated with SNP in immunoblot, and pretreatment of the cells with chemical inhibitors of MAPKs inhibited cytotoxicity in cell viability assays. We further confirmed this involvement by

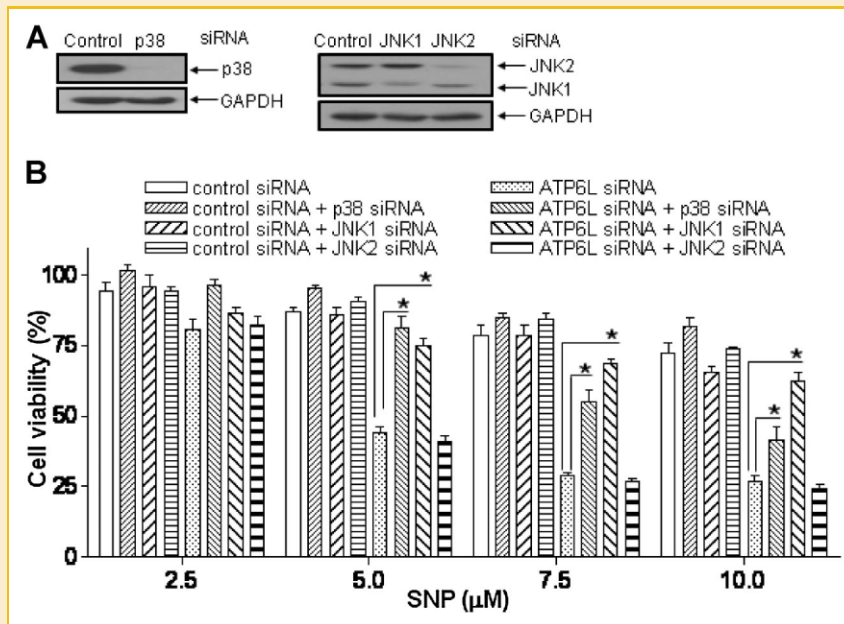


Fig. 7. Involvement of p38 and JNK in the SNP-induced cytotoxicity in ATP6L siRNA-transfected cells. A: Efficiency of silencing gene expression was examined after transfection of p38, JNK1, or JNK2 siRNA by immunoblot analysis of protein lysates. GAPDH was used as loading controls. B: SNP-induced cytotoxicity was examined by cointroduction of ATP6L siRNA with p38, JNK1, or JNK2 siRNA into cells. The cointroduced cells were treated with SNP for 6 h in the presence of BSO. Cell viability was determined by an MTT reduction assay. The data represent the mean \pm SEM of four independent experiments. * $P < 0.05$ versus the values in the cells transfected with ATP6L siRNA alone.

cotransfection of the MAPK and ATP6L siRNAs into cells. We could not find data supporting the interactions between p38 and JNK signaling in immunoblot analyses of the cotransfected cells. Pretreatment of the cells combined with p38 and JNK inhibitors showed the effect of additive inhibition of the cytotoxicity (data not shown).

In our study, pretreatment of the cells with zVAD-fmk did not affect the cell viability. Change of apoptotic parameters in the cells was not shown either in flow cytometry with annexin V or in immunoblot analyses with antibodies against caspase-3 and PARP. Recent studies demonstrated that increase of intracellular ROS can induce autophagic cell death [Azad et al., 2009]. We, therefore, examined the autophagic markers in ATP6L siRNA-transfected cells treated with SNP. Conversion of LC3 increased in the cells, but it was inhibited by pretreatment with DFO. The findings imply that autophagic cell death processes were activated in the cells treated with SNP. An interesting report recently suggested the importance of intracellular GSH level in determination of apoptotic and autophagic cell death [Itoh et al., 2009]. Euphalin A induces autophagic cell death in HL 60 cells via an increase of intracellular ROS and a decrease of the GSH level, but the cell death is converted to apoptotic by GSH supplementation. To confirm the involvement of autophagic cell death in ATP6L siRNA-transfected cells treated with SNP, we cointroduced ATP6L siRNA with Atg5 or beclin-1 siRNA into the cells. Analyses of Atg5 siRNA-cotransfected cells showed inhibition of the cytotoxicity and LC3 conversion and inhibition of the p38 and JNK activations. However, cointroduction of ATP6L siRNA with beclin-1 siRNA into cells did not affect the

cytotoxicity. We do not have data supporting the molecular mechanism of the autophagic process independent of beclin-1. Recent studies demonstrated that non-canonical autophagic cell death independent of beclin-1 is induced by resveratrol or by ROS via JNK and ERK activation [Scarlati et al., 2008; Wong et al., 2010].

Most reports described that activation of p38 and JNK MAPKs occurs upstream of autophagy initiation. In contrast to these findings, we found that activation of the MAPKs was inhibited by cointroduction of Atg5 and ATP6L siRNAs. Possible explanation for the discrepancy might be related to differences in cell type, stimuli, or intracellular GSH levels used in the studies. A report recently described that activation of JNK occurs downstream of autophagy induction in bax/bak double-knockout cells treated with etoposide or staurosporine [Shimizu et al., 2010]. Another report described the activation of p38 involved in the regulation of autophagosomal maturation step [Corcelle et al., 2007]. But it is unclear that our data on the involvement of p38 and JNK correspond to the reports in the precise working step in autophagic processes.

In the study, we found that ATP6L siRNA-transfected glial cells were more sensitive to SNP than control cells under GSH-depleted conditions, and this was independent of the V-ATPase complex protein. Of the SNP components, iron dominantly contributed to the cytotoxicity via ROS generation leading to autophagic cell death, in which activations of p38 and JNK were independently involved in the autophagic processes. These data suggest that ATP6L has a protective role against SNP-induced autophagic cell death via inhibition of JNK and p38 in GSH-depleted glial cells.

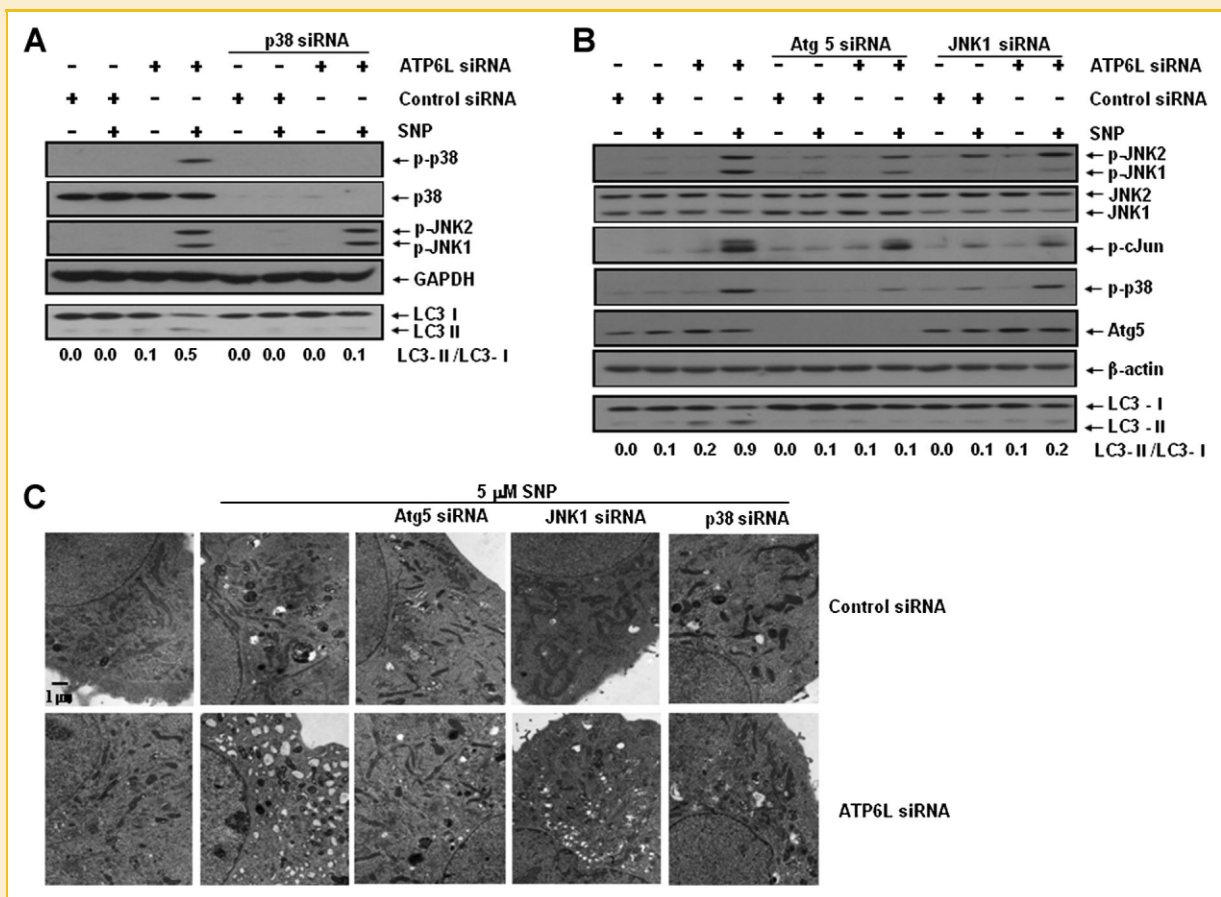


Fig. 8. SNP-induced autophagic cell death via activations of p38 and JNK in ATP6L siRNA-transfected cells. A,B: ATP6L siRNA were transfected or cotransfected with p38, Atg5, or JNK1 siRNA into cells. The cells were treated with 5 μ M SNP for 2 h in the presence of BSO. Activation of p38 and JNK and LC3 conversion were examined by immunoblot analysis of the protein lysates. The LC3 conversion was expressed in a ratio of LC3-II to LC3-I as determined by densitometry of the immunoblots. β -actin and GAPDH were used as loading controls. C: SNP-induced autophagic vacuoles in ATP6L siRNA-transfected cells were examined. siRNA-transfected cells were treated with 5 μ M SNP for 2 h in the presence of BSO, and the ultrastructural morphology of the cells was examined by transmission electron microscopy, as described in the Materials and Methods Section. The roles of Atg5 and MAPKs in ATP6L siRNA-transfected cells were also examined with cotransfection of siRNAs targeting the gene. Scale bar: 1 μ m.

ACKNOWLEDGMENTS

This work was supported by the Korea Science and Engineering Foundation (KOSEF) through the MRC for Cell Death Disease Research Center (CDDRC) at The Catholic University of Korea (R13-2002-005-03002-0). We thank professor Ki-Wug Sung for technical assistance.

REFERENCES

- Andresson T, Sparkowski J, Goldstein DJ, Schlegel R. 1995. Vacuolar H⁺-ATPase mutants transform cells and define a binding site for the papillomavirus E5 oncoprotein. *J Biol Chem* 270:6830–6837.
- Ashby AD, Meagher L, Campo MS, Finbow ME. 2001. E5 transforming proteins of papillomaviruses do not disturb the activity of the vacuolar H⁺-ATPase. *J Gen Virol* 82:2353–2362.
- Azad MB, Chen Y, Gibson SB. 2009. Regulation of autophagy by reactive oxygen species (ROS): Implications for cancer progression and treatment. *Antioxid Redox Signal* 11:777–790.
- Blackburn RV, Galoforo SS, Berns CM, Motwani NM, Corry PM, Lee YJ. 1998. Differential induction of cell death in human glioma cell lines by sodium nitroprusside. *Cancer* 82:1137–1145.
- Bragin DE, Zhou B, Ramamoorthy P, Muller WS, Connor JA, Shi H. 2010. Differential changes of glutathione levels in astrocytes and neurons in ischemic brains by two-photon imaging. *J Cereb Blood Flow Metab* 30:734–738.
- Byun YJ, Lee SB, Kim DJ, Lee HO, Son MJ, Yang CW, Sung KW, Kim HS, Kwon OJ, Kim IK, Jeong SW. 2007. Protective effects of vacuolar H⁺-ATPase c on hydrogen peroxide-induced cell death in C6 glioma cells. *Neurosci Lett* 425:183–187.
- Byun YJ, Kim SK, Kim YM, Chae GT, Jeong SW, Lee SB. 2009. Hydrogen peroxide induces autophagic cell death in C6 glioma cells via BNIP3-mediated suppression of the mTOR pathway. *Neurosci Lett* 461:131–135.
- Cardaci S, Filomeni G, Rotilio G, Ciriolo MR. 2008. Reactive oxygen species mediate p53 activation and apoptosis induced by sodium nitroprusside in SH-SY5Y cells. *Mol Pharmacol* 74:1234–1245.
- Corcelle E, Djerbi N, Mari M, Nebout M, Fiorini C, Fenichel P, Hofman P, Poujeol P, Mograbi B. 2007. Control of the autophagy maturation step by the MAPK ERK and p38: Lessons from environmental carcinogens. *Autophagy* 3:57–59.
- Coyle JT, Puttfarcken P. 1993. Oxidative stress, glutamate, and neurodegenerative disorders. *Science* 262:689–695.
- Crider BP, Xie XS, Stone DK. 1994. Bafilomycin inhibits proton flow through the H⁺ channel of vacuolar proton pumps. *J Biol Chem* 269:17379–17381.

- Dringen R. 2000. Metabolism and functions of glutathione in brain. *Prog Neurobiol* 62:649–671.
- Feeney CJ, Frantseva MV, Carlen PL, Pennefather PS, Shulyakova N, Shniffer C, Mills LR. 2008. Vulnerability of glial cells to hydrogen peroxide in cultured hippocampal slices. *Brain Res* 1198:1–15.
- Friederich JA, Butterworth JFt. 1995. Sodium nitroprusside: Twenty years and counting. *Anesth Analg* 81:152–162.
- Halliwell B. 1992. Reactive oxygen species and the central nervous system. *J Neurochem* 59:1609–1623.
- Itoh T, Ohguchi K, Nozawa Y, Akao Y. 2009. Intracellular glutathione regulates sesquiterpene lactone-induced conversion of autophagy to apoptosis in human leukemia HL60 cells. *Anticancer Res* 29:1449–1457.
- Jang H, Choi SY, Cho EJ, Youn HD. 2009. Cabin1 restrains p53 activity on chromatin. *Nat Struct Mol Biol* 16:910–915.
- Kawasaki T, Kitao T, Nakagawa K, Fujisaki H, Takegawa Y, Koda K, Ago Y, Baba A, Matsuda T. 2007. Nitric oxide-induced apoptosis in cultured rat astrocytes: Protection by edaravone, a radical scavenger. *Glia* 55:1325–1333.
- Keller A, Mohamed A, Drose S, Brandt U, Fleming I, Brandes RP. 2004. Analysis of dichlorodihydrofluorescein and dihydrocalcein as probes for the detection of intracellular reactive oxygen species. *Free Radic Res* 38:1257–1267.
- Kim EK, Choi EJ. 2010. Pathological roles of MAPK signaling pathways in human diseases. *Biochim Biophys Acta* 1802:396–405.
- Kim HJ, Tsoy I, Park MK, Lee YS, Lee JH, Seo HG, Chang KC. 2006. Iron released by sodium nitroprusside contributes to heme oxygenase-1 induction via the cAMP-protein kinase A-mitogen-activated protein kinase pathway in RAW 264.7 cells. *Mol Pharmacol* 69:1633–1640.
- Kubota S, Seyama Y. 2000. Overexpression of vacuolar ATPase 16-kDa subunit in 10T1/2 fibroblasts enhances invasion with concomitant induction of matrix metalloproteinase-2. *Biochem Biophys Res Commun* 278:390–394.
- Lin HJ, Herman P, Kang JS, Lakowicz JR. 2001. Fluorescence lifetime characterization of novel low-pH probes. *Anal Biochem* 294:118–125.
- Livak KJ, Schmittgen TD. 2001. Analysis of relative gene expression data using real-time quantitative PCR and the $2^{-\Delta\Delta Ct}$ Method. *Methods* 25:402–408.
- Makar TK, Nedergaard M, Preuss A, Gelbard AS, Perumal AS, Cooper AJ. 1994. Vitamin E, ascorbate, glutathione, glutathione disulfide, and enzymes of glutathione metabolism in cultures of chick astrocytes and neurons: Evidence that astrocytes play an important role in antioxidative processes in the brain. *J Neurochem* 62:45–53.
- Mancardi D, Ridnour LA, Thomas DD, Katori T, Tocchetti CG, Espey MG, Miranda KM, Paolocci N, Wink DA. 2004. The chemical dynamics of NO and reactive nitrogen oxides: A practical guide. *Curr Mol Med* 4:723–740.
- Rabkin SW, Kong JY. 2000. Nitroprusside induces cardiomyocyte death: Interaction with hydrogen peroxide. *Am J Physiol Heart Circ Physiol* 279:H3089–H3100.
- Ramakrishna Rao DN, Cederbaum AI. 1996. Generation of reactive oxygen species by the redox cycling of nitroprusside. *Biochim Biophys Acta* 1289:195–202.
- Rauhala P, Khaldi A, Mohanakumar KP, Chiueh CC. 1998. Apparent role of hydroxyl radicals in oxidative brain injury induced by sodium nitroprusside. *Free Radic Biol Med* 24:1065–1073.
- Reiter RJ. 1995. Oxidative processes and antioxidative defense mechanisms in the aging brain. *FASEB J* 9:526–533.
- Santic M, Asare R, Skrobonja I, Jones S, Abu Kwaik Y. 2008. Acquisition of the vacuolar ATPase proton pump and phagosome acidification are essential for escape of *Francisella tularensis* into the macrophage cytosol. *Infect Immun* 76:2671–2677.
- Scarlati F, Maffei R, Beau I, Codogno P, Ghidoni R. 2008. Role of non-canonical Beclin 1-independent autophagy in cell death induced by resveratrol in human breast cancer cells. *Cell Death Differ* 15:1318–1329.
- Schapiro F, Sparkowski J, Adduci A, Supryniewicz F, Schlegel R, Grinstein S. 2000. Golgi alkalization by the papillomavirus E5 oncoprotein. *J Cell Biol* 148:305–315.
- Shimizu S, Konishi A, Nishida Y, Mizuta T, Nishina H, Yamamoto A, Tsujimoto Y. 2010. Involvement of JNK in the regulation of autophagic cell death. *Oncogene* 29:2070–2082.
- Simonian NA, Coyle JT. 1996. Oxidative stress in neurodegenerative diseases. *Annu Rev Pharmacol Toxicol* 36:83–106.
- Skinner MA, Wildeman AG. 1999. beta(1) integrin binds the 16-kDa subunit of vacuolar H⁺-ATPase at a site important for human papillomavirus E5 and platelet-derived growth factor signaling. *J Biol Chem* 274:23119–23127.
- Son MJ, Lee SB, Byun YJ, Lee HO, Kim HS, Kwon OJ, Jeong SW. 2010. Sodium nitroprusside induces autophagic cell death in glutathione-depleted osteoblasts. *J Biochem Mol Toxicol* 24:313–322.
- Takuma K, Baba A, Matsuda T. 2004. Astrocyte apoptosis: Implications for neuroprotection. *Prog Neurobiol* 72:111–127.
- Wang J, Fillebeen C, Chen G, Andriopoulos B, Pantopoulos K. 2006. Sodium nitroprusside promotes IRP2 degradation via an increase in intracellular iron and in the absence of S nitrosylation at C178. *Mol Cell Biol* 26:1948–1954.
- Wong CH, Iskandar KB, Yadav SK, Hirpara JL, Loh T, Pervaiz S. 2010. Simultaneous induction of non-canonical autophagy and apoptosis in cancer cells by ROS-dependent ERK and JNK activation. *PLoS ONE* 5:e9996.
- You H, Jin J, Shu H, Yu B, De Milito A, Lozupone F, Deng Y, Tang N, Yao G, Fais S, Gu J, Qin W. 2009. Small interfering RNA targeting the subunit ATP6L of proton pump V-ATPase overcomes chemoresistance of breast cancer cells. *Cancer Lett* 280:110–119.
- Zeevalk GD, Bernard LP, Nicklas WJ. 1998. Role of oxidative stress and the glutathione system in loss of dopamine neurons due to impairment of energy metabolism. *J Neurochem* 70:1421–1430.